3-3-2018

The Role of Supervised Learning in the Decision Process to Fair Trade US Municipal Debt

Gordon H. Dash jr
University of Rhode Island, ghdash@uri.edu

Nina Kajiji

Domenic Vonella

Citation/Publisher Attribution

Dash, G. H., Kajiji, N., & Vonella, D. (2018). The role of supervised learning in the decision process to fair trade US municipal debt. *EURO Journal on Decision Processes*, 1-2, 139-168. doi: 10.1007/s40070-018-0079-2
Available at: http://dx.doi.org.uri.idm.oclc.org/10.1007/s40070-018-0079-2

EURO Journal on Decision Processes

The Role of Supervised Learning in the Decision Process to Fair Trade U.S. Municipal Debt

--Manuscript Draft--

Manuscript Number:	EJDP-D-17-00018
Full Title:	The Role of Supervised Learning in the Decision Process to Fair Trade U.S. Municipal Debt
Article Type:	S.I. : Financial Decision Support
Corresponding Author:	Gordon H Dash, PhD University of Rhode Island Kingston, RI UNITED STATES
Corresponding Author Secondary Information:	
Corresponding Author's Institution:	University of Rhode Island
Corresponding Author's Secondary Institution:	
First Author:	Gordon H Dash, PhD
First Author Secondary Information:	
Order of Authors:	Gordon H Dash, PhD
	Nina Kajiji, PhD
	Domenic Vonella
Order of Authors Secondary Information:	
Funding Information:	
Abstract:	Determining a fair price and an appropriate timescale to trade municipal debt is a complex decision. This research uses big data informatics to explore transaction characteristics and trading activity of investment grade U.S. municipal bonds. Using the relatively recent data stream distributed by the Municipal Securities Rulemaking Board (MSRB) to Thomson Reuters Municipal Markets Division (MMD) we provide an institutional summary of market participants and their trading behavior. Subsequently, we focus on a sample of AAA bonds to derive a new methodology to estimate a trade weighted benchmark municipal yield curve. The methodology integrates the study of ridge regression, artificial neural networks, and support vector regression. We find an enhanced radial basis function artificial neural network outperforms alternate methods used to estimate municipal term structure. This result forms the foundation for establishing a decision theory on optimal municipal bond trading. Using multivariate modeling where the target variables are defined by three popular liquidity measures, we investigate the proposed decision theory by estimating weekly production-theoretic bond liquidity returns-to-scale. Across the three liquidity measures and for almost all weeks investigated bond trading liquidity is elastic with respect to the modeled factors. This finding leads us to conclude that an optimal trading policy for municipal debt can be implemented on a weekly timescale using the elasticity estimates of bond price, trade size, risk, days-to-maturity and the macroeconomic influences of labor in the workforce and building activity.
Suggested Reviewers:	Gerhard-Wilhelm Weber, PhD Professor gweber@metu.edu.tr Expertise in AI, computational finance and learning methods
	Tiny du Toit Tiny.duToit@nwu.ac.za Expert in radial basis function artificial neural networks
	Luciana Guimaraes

	luciana.guimaraes@cirrelt.ca Expertise in decision-making and OR for development

The Role of Supervised Learning in the Decision Process to Fair Trade U.S. Municipal Debt

Gordon H. Dash[a]
Nina Kajiji[b]
Domenic Vonella[c]

[a]*Finance and Decision Sciences Area, College of Business Administration, University of Rhode Island; and, Faculty, Interdisciplinary Neuroscience Program, University of Rhode Island*

[b] *Department of Computer Science and Statistics, University of Rhode Island*
Principal, The NKD Group, Inc., Providence, RI

[c] *Municipal Market Division, Thomson Reuters, Boston*

Submitted for publication consideration in the Feature Issue on "Financial Decision Support", *Euro Journal on Decision Processes**, 30-July-2017. Please address all correspondence to:* *ghdash@uri.edu*
ORCID=ghdash

The Role of Supervised Learning in the Decision Process to Fair Trade U.S. Municipal Debt

Abstract

Determining a fair price and an appropriate timescale to trade municipal debt is a complex decision. This research uses big data informatics to explore transaction characteristics and trading activity of investment grade U.S. municipal bonds. Using the relatively recent data stream distributed by the Municipal Securities Rulemaking Board (MSRB) to Thomson Reuters Municipal Markets Division (MMD) we provide an institutional summary of market participants and their trading behavior. Subsequently, we focus on a sample of AAA bonds to derive a new methodology to estimate a trade weighted benchmark municipal yield curve. The methodology integrates the study of ridge regression, artificial neural networks, and support vector regression. We find an enhanced radial basis function artificial neural network outperforms alternate methods used to estimate municipal term structure. This result forms the foundation for establishing a decision theory on optimal municipal bond trading. Using multivariate modeling where the target variables are defined by three popular liquidity measures, we investigate the proposed decision theory by estimating weekly production-theoretic bond liquidity returns-to-scale. Across the three liquidity measures and for almost all weeks investigated bond trading liquidity is elastic with respect to the modeled factors. This finding leads us to conclude that an optimal trading policy for municipal debt can be implemented on a weekly timescale using the elasticity estimates of bond price, trade size, risk, days-to-maturity and the macroeconomic influences of labor in the workforce and building activity.

Keywords: Decision Theory, Municipal Bonds; Supervised Learning, and Production Theory

JEL Codes: C15, C45, C55, C58

1. Introduction

Market participants believe the primary market for U.S. municipal bonds is efficient for the supply of funds to municipalities and state governments. But, by participant consensus, many argue this same market is widely inefficient in meeting its secondary function of promoting the price-efficient trading of municipal debt. One explanatory reason for this perceived secondary market failure is the lack of a benchmark term structure (yield) curve. The absence of a bellwether curve retards the ability of market participants to compare yields of traded bonds to a generally accepted market-wide snapshot. Absent a benchmark it is all too possible that funds are trapped in the market thereby causing liquidity and pricing distortions. This characterization begs a question about whether the decision to trade securities in the U.S. municipal market can be made efficiently and in a timely manner.

Bond liquidity, credit rating, along with macroeconomic events are some of the important features that influence the decision to trade a fixed income instrument at a fair price. To increase market transparency and to encourage research about municipal debt liquidity and trading activity, in 2001 under the direction of the Securities and Exchange Commission (SEC), the Municipal Securities Rulemaking Board (MSRB) mandated all-trade reporting for the municipal market. Today, the MSRB manufactures and distributes a delayed trade tape (or, a digital representation thereof). This significant achievement was designed to improve the decision process for describing, predicting and trading municipal bonds across all rating classes. Coincidentally and somewhat unexpectedly, the sudden availability of voluminous fragmented trade data brought about a new informational complexity in decision-making as market participants confronted "Big Data" in the municipal trading.

In a rational market, an optimal trading decision is based on a descriptive theory that incorporates the municipal bond valuation matrix. A study of this decision process is dependent upon the enumeration of a generally accepted benchmark yield curve that best captures the valuation of all traded bonds. Currently, the Thomson Reuters Municipal Markets Division (MMD) set of credit differentiated municipal bond curves serve as the leading, if not benchmark, term structures for the industry. The term structure characterized by these curves is accumulated from a daily informal survey. Hence, the MMD curves do not use an objective sampling of all, or some subset, of available market data. Research contributions on this topic by Vasicek (1977), and Cox, Ingersoll and Ross (1985) were among the first to introduce the need for fixed-income markets to rely on an objectively defined term structure models (see, (Dai and Singleton 2000)) for a review and classification of the affine models study during this era). While objective econometric methodology has successfully fit term structure models, the early approaches did not consider the statistical link between yield factors and macroeconomic forces.

We can divide subsequent research efforts into alternate methodological strains. One strain is generally referred to as the 'segmented-loading' term structure model (SL). This approach focuses on splitting the original set of maturities into a group of segments where local factors become time-varying coefficients from a linear combination of the individual basis functions. The attractiveness of this approach lies in the fact that it is computationally flexible when explaining how shocks to local factors affect only those maturities specific to each segment (Almeida et al. 2013). By way of example, motivated by the Preferred-Habitat theory, Bowsher and Meeks (2013) employed an exponential SL model with piecewise cubic spline post smoothing to demonstrate that local shocks are important determinants of yield curve dynamics.

Of interest to the research goals of this paper is a competing strain of research that focuses on regime switching models (RS). RS models are known to map historical data efficiently and generate robust out-of-sample forecasts. Findings report that at the time of a regime shift, non-switching models understate fluctuations in excess returns and overstate excess returns and volatility factor risk premiums (Dai et al. 2007). Newer findings demonstrate a preference for a two regime model (Xiang and Zhu 2013). Accepted practice expresses a RS model as an extension to the well-known Nelson-Siegel (NS) term structure model (Nelson and Siegel 1987). The NS model is based upon three factors: a long-run component to capture the long-run interest level; a short-term component that decays monotonically; and, a medium term component that starts at zero (0), increases, then decays to zero. When a fourth factor was added to account for dynamic regime switching, Levant and Ma (2013) found the additional factor's loading parameter and conditional volatilities showed switching significance (in contrast to the conditional means previously evaluated in the literature). NS-based models also include extensions to account for macroeconomic factors. Research contributions by Ang and Piazzesi (2003), Diebold, Rudebush, and Aruoba (2006), Moench (2008), and De Pooter, et. al. (2010) provide confirmatory evidence of the importance of macroeconomic influences. Gonzalez-Rozada, et.al. (2012) shows how macroeconomic factors significantly affect the level, slope, and curvature of the government bond term structure.[1] Some of these same research methodologies have been used to investigate the municipal term structure. For example, questions about the slope of the curve were investigated by Kalotay, et.al. (2008) and Daniels and Ejara (2009). Studies on municipal debt credit worthiness are also represented in the literature (Olej and Hájek 2009) and (Lin et al. 2010).

In this paper we focus we form a descriptive theory to explain the decision process of trading municipal debt with a fair price on a timely basis. The evolution of the theoretical approach takes place in two steps. The first is to develop an AI-inspired benchmark yield curve based on the Nelson-Siegel (NS) term structure model (Nelson and Siegel 1987). The AI-inspired modeling extension is used to design and deploy a new benchmark municipal yield curve; a new curve methodology that natively captures both regime shifts and macroeconomic pricing factors. The second step in developing a new descriptive decision theory for trading municipal debt is to

[1] Creal and Wu (2014) provide an alternative research strain based on affine models to demonstrate how spanned stochastic volatility captures either the cross-section of yields or the fitted volatility .

invoke a production theoretic model to estimate individual bond liquidity (Illiquidity) scale elasticity metrics for the driving production factors. These factors include bond fundamentals, information from a benchmark yield spread, and representative economic factors.

The paper proceeds as follows. In section 2 we describe market characteristics of municipal bond trades. Alternative supervised learning models for term structure mapping are developed throughout section 3. Section 4 presents model estimation results. In section 5 we present production-theoretic traded bond liquidity factor scale-elasticity metrics. The metrics are related to the trading decision process. A summary and conclusion closes the paper in section 6.

2. Market Characteristics of Municipal Bond Trades

The first step in our quest to replace systematic biases and heuristics in the trading of municipal bonds is to evolve a descriptive theory for the pricing of an all-trade benchmark term structure across rating classes. Currently, the Thomson Reuters Municipal Markets Division (MMD) set of credit differentiated municipal bond curves serve as the leading, if not benchmark, term structures for the industry. Accordingly, in this section we begin the process of evolving a new descriptive theory empirically examining the market composition of daily trades as reported on the MSRB data tape.

2.1 Data Munging and Extraction

In February-2015 Luis A. Aguilar, Commissioner of the Securities and Exchange Commission, updated regulatory concerns about the need to make the U.S. municipal securities market more transparent, liquid and fair rather than "*excessively opaque, illiquid, and decentralized*" (Aguilar 2015). Aguilar challenged the Municipal Rule Making Board (MSRB) to produce a series of cumulative changes that would, over time, enhance all aspects of efficiency. Importantly, his decree called for the MSRB to enhance muni market structure by disclosing pricing and reference information on customer confirmations for transactions. The dissemination of the MSRB trade tape is a partial response to this challenge. Today, the MSRB reports about 40,000 municipal bond trades via the trade tape.

As a relatively new big data product, upon inspection researchers are not surprised to encounter inaccurate and missing data. Errors and omissions include, missing effective maturity date, negative coupons, missing market price, etc. Trades of bonds bearing error data are not included in our study sample. Given the need to evolve a new benchmark term structure we compute a discrete term structure from the dynamic data. Additionally, in recognition of confidentiality requirements, any trade with a trade size of 1 million dollars (1M) or above is recorded in the sample study as a 1M trade.

As stated previously a primary study goal is to develop a benchmark trade-weighted yield curve to improve the efficiency of fair pricing in the industry. The process begins with munged data covering 2012-May to 2014-February inclusive. Subsequently, we exclude individual bond trades from the study for any one of the following reasons: a) bond is priced to PUT; b) bond interest payments are taxable; c) the bond has a variable rate of interest; d) bond does not have a third-party investment grade (IG) credit rating (BBB or higher); e) bond is a zero coupon bond; and, f) computed bond maturity is less than 1 year or greater than 30 years. We also note each reported trade is tagged as: a sale to a customer, a purchase from a customer, or a dealer-to-dealer transaction.

2.2 Market Activity for Investment Grade Municipal Bonds

For big data management, the filter was applied to bond trades recorded during the middle month of each calendar quarter (February, May, August, and November) starting in May 2012 and ending in February 2014. The number and percent density of monthly trades for the study period are presented in table 1.

Table 1. Number and percent of trades for investment grade bond classification

	May-12	Aug-12	Nov-12	Feb-13	May-13	Aug-13	Nov-13	Feb-14
AAA	20,218	42,894	40,826	45,400	49,912	64,046	48,961	45,112
	8.44%	8.95%	8.74%	9.70%	9.73%	8.89%	9.15%	9.61%
AA	137,548	259,981	264,548	231,622	253,394	333,888	247,733	224,702
	57.43%	54.27%	56.61%	49.50%	49.42%	46.33%	46.29%	47.87%
A	54,326	109,025	107,957	146,039	164,914	264,687	185,848	158,525
	22.68%	22.76%	23.10%	31.21%	32.16%	36.73%	34.72%	33.77%
BBB	27,422	67,107	54,025	44,826	44,506	58,038	52,659	41,045
	11.45%	14.01%	11.56%	9.58%	8.68%	8.05%	9.84%	8.74%
TOTAL	**239,514**	**479,007**	**467,356**	**467,887**	**512,726**	**720,659**	**535,201**	**469,384**

In the municipal bond market there are three important ways a trade is executed. These are: a) between two dealers which is labeled as “Dealer to Dealer”; b) dealer selling to a customer which is labeled as “Purchase by Customer”; and c) when a dealer purchases from a customer which is labeled as “Sale by Customer”. Next we investigate the trading behavior for the investment grade trades. As shown in figure 1, for the most part, until May-2013 the trading levels by each group remain relatively stable. Between May-2013 and August-2013 the indicator for both ‘interdealer’ and ‘purchases by customer’ show a drop in trading. Over the corresponding time period ‘sale by customer’ increases sharply. Without delving into further analytical review, we note this trend coincides with the June-2013 policy announcement by the United States Federal Reserve to taper QE policies.

<< Insert Figure 1 here >>

2.3 Daily AAA Trades

For practical reasons, the majority of our analysis will focus on the AAA panel of table 1. In this credit class the percentage of filtered bonds traded on any given day remains fairly constant across all days of the month and all months for the study period. By contrast, the percentage of filtered AA bonds traded relative to all trades shows a decline over the study period. The inverse is true for the filtered A bonds. The number of AA and A bonds traded has an up and down relationship with a sharp spike in Aug-2013. Taken together filtered AA and A rated bonds demonstrate more variability in their trading characteristics when compared to both AAA and BBB rated bonds. The yields reported in this section are yield-to-worst (YTW) and are not subjected to outlier detection. The provided industry AAA benchmark is from MMD.

2.4 AAA Term Yields by Maturity

Table 2 reports dispersion data of the YTW of the traded bonds for 01-May-2012 as well as for the month of May 2012. The range of yield spreads stands out for both the day- and month-view. To exemplify we focus on the 5 year spot of the term structure for 01-May-2012. At this maturity point the spread is noticeable and comparatively broad. This one-day visualization provides simple evidence of the possibility traders may face yield spreads over or approaching 600 basis points on maturities up to 10 years. On this day, traded yields ranged from a low 1.29% (30yr spot) to a high of 5.16% (5yr spot). Within the monthly reported data, the yield range spanned from a low of 2.85% (30yr spot) to a high of 6.22% (1yr spot). The hypothesized upward sloping term structure is in evidence. As the analysis proceeds towards a discussion on switching regimes, we note the 6.13% spike in yield range at the 10-year spot. Otherwise, the range is continually decreasing over the entire term structure. Table 3, provides a similar analysis for Feb 2014. In 2014 the spike anomaly occurs at the 20-year spot.

Table 2. Range of dispersion of the AAA yield-to-worst for May 2012

	May 1st, 2012				**Month of May, 2012**			
Total Trades	887				20218			
# of Unique bonds	775				1022			
Minimum Yield	0.03% @ 7 year maturity				0.01% @ 12 year maturity			
Maximum Yield	5.79% @ 2 year maturity				11.80% @ 3 year maturity			
	Min	**Max**	**Median**	**Range**	**Min**	**Max**	**Median**	**Range**
1yr	0.05%	2.84%	0.70%	2.79%	0.04%	6.26%	0.65%	6.22%
5yr	0.55%	5.71%	1.21%	5.16%	0.20%	5.71%	1.17%	5.69%
7yr	0.03%	2.48%	1.62%	2.45%	0.03%	5.31%	1.55%	5.28%
10yr	0.51%	3.21%	1.85%	2.70%	0.23%	6.36%	2.00%	6.13%
15yr	2.04%	3.57%	2.72%	1.53%	0.13%	5.17%	2.55%	5.04%
20yr	0.78%	3.98%	3.11%	3.20%	0.29%	5.02%	2.70%	4.73%
30yr	2.49%	3.78%	3.22%	1.29%	1.00%	3.85%	2.18%	2.85%

Table 3. Range of Dispersion of the AAA Yield-to-Worst for Feb 2014

	Feb 3rd, 2014				Month of Feb, 2014			
Total Trades	2433				45112			
# of Unique Bonds	1006				8297			
Minimum Yield	0.17% @ 1 year maturity				0.00% @ 1 year maturity			
Maximum Yield	5.59% @ 4 year maturity				6.38% @ 11 year maturity			
	Min	**Max**	**Median**	**Range**	**Min**	**Max**	**Median**	**Range**
1yr	0.17%	1.87%	0.47%	1.70%	0.00%	5.35%	5.00%	5.35%
5yr	0.50%	3.58%	1.34%	3.08%	0.07%	5.24%	1.33%	5.17%
7yr	0.85%	3.97%	2.06%	3.12%	0.01%	5.33%	2.03%	5.32%
10yr	0.23%	4.94%	2.65%	4.71%	0.23%	4.94%	2.57%	4.71%
15yr	1.20%	4.55%	3.01%	3.35%	0.59%	5.12%	3.18%	4.53%
20yr	1.45%	4.82%	3.39%	3.37%	0.01%	5.11%	3.54%	5.10%
30yr	-	-	-	-	3.45%	4.55%	3.77%	1.10%

The asymmetric nature of the dispersion is not just a one-day phenomenon. Covering all trading days in the month of May, figures 2 and 3 use the non-parametric box-and-whiskers (BW) plot at maturity points of 1, 2, 5, 7, 10, 15, 20, 25, and 30 years to visually demonstrate the asymmetric dispersion of daily trade yields in 2012 and 2014, respectively. The lines extending vertically from the boxes (the whiskers) indicate variability outside the upper- and lower-quartiles; an indication that may result in the identification of an extreme yield outlier. We note that box-and-whisker charts for all months of the study period are provided.[2]

<< Insert Figure 2 here >>
<< Insert Figure 3 here >>

The dispersion results presented to this point lead to a conjecture about the level, slope, and curvature of the daily municipal term structure. To punctuate the BW comparative analysis figures 4 and 5 show daily term structure for the months of May-2012 and Feb-2914, respectively.[3] In an efficient market, the charts would show the characteristic smooth shape of an upward sloping yield curve. The 'wrinkles' in the chart provide additional evidence of municipal pricing inefficiency; or, following Daniels and Ejara (2009) in their study of general obligation and revenue bonds, the wrinkles represent a form of irrational to random behavior.

<< Insert Figure 4 here >>
<< Insert Figure 5 here >>

These findings lend credence to the belief that, in general, traders seek to develop a visual "feel" for the market in which they trade Steenbarger (2003). A more logical approach for the data scientist is to invoke a "computing machine" to reconcile the vagaries of human decision-making and the economic theories of rational behavior.

[2] For a complete listing see: http://bit.ly/2eZvyY5
[3] All term structure curves are available at: http://bit.ly/2eZvyY5

The observations provided thus far lead to interesting questions about decision process required to make trade decisions in the secondary municipal bond market at a fair price and on a timely basis. For example, what is the impact of market liquidity on traded yields? Does the time-varying dispersion of traded yields influence trading on a given day or week? Is daily liquidity induced (retarded) by changes in macroeconomic influences? To address these questions and more the next section of the paper proposes a hierarchical model-building methodology to estimate an all-in-all trade weighted (trade size) benchmark yield curve for the U.S. municipal bond market.

3. Alternative Models for Term Structure Mapping

This section turns its attention to extending the NS model by applying AI mapping to yields estimated from MSRB reported trades. To establish the statistical domination of the newly designed curve, we compare and contrast alternate approaches. Linear regression based approaches tend to dominate the extant literature (see, (De Pooter 2007; Diebold and Li 2006; Fabozzi et al. 2005)). But, in an effort to improve the shape parameter Annaert, et. al. (2010) introduced ridge regression. Even with this extension, all variants of regression-based modeling still exhibit ill-behaved parameter estimates characterized by relatively large variances from excessive multicollinearity.

Based on the findings provided, this paper implements a comparative analysis of four alternate mapping models. We begin with a simple piecewise approximation using a B-Spline technique (not to be confused with the more popular Bezier curve/surface). Included in the comparative analysis is a ridge regression model. Subsequently, we introduce two alternate modeling methodologies that are new to the mapping of bond yield term structure. One is an artificial intelligence-inspired radial basis function artificial neural network (RANN) – the K3-RANN (Kajiji 2001). The other model uses the support vector machine regression (SVR) method.

3.1 Removal of Extreme YTW Outliers

Over the study period, the data presented in table 1 reports 357,369 AAA-rated trades. As discussed in section 2, these trades include some extreme outliers. Owing to the existence of outliers, at a given discrete maturity point (t) we compute a traditional z-score or a modified z-score (Iglewicz and Hoaglin 1993) as follows:

$$z_i = \begin{cases} \dfrac{\left(x_{it} - \bar{x}_t\right)}{s_t} & n_t \geq 20 \\[2ex] \dfrac{0.6745\left(x_{it} - \tilde{x}_t\right)}{MAD_t} & 5 \leq n_t < 20 \end{cases} \tag{1}$$

In equation 1 above, for the i^{th} trade at the t^{th} maturity, x is the YTW, n is the number of trades, $\bar{x}$ denotes the average yield, s is the standard deviation of the yields, MAD denotes the median absolute deviation of yields, and $\tilde{x}$ denotes the median yield. We statistically eliminate outlier yields if the z-score is > $|1.96|$ (or outside the 95% confidence interval) or if the modified z-score is > |3.5|. The outlier test is not performed for $n_t < 5$.

3.2 Trade-Weighted Yields

The new term structure is designed to reflect yields modified by their daily trade size impact on market valuation. For each trade point we compute the associated trade-weighted YTW as follows:

$$y_{it} = x_{it}\left(\frac{v_{it}}{\sum_{j=1}^{n_t} v_{jt}}\right). \tag{2}$$

In equation 2 above for the i^{th} trade at the t^{th} maturity x_{it} is the unweighted YTW, v_{it} is the trade size, and the trade-weighted yield is represented by y_{it}. The number of trades at a maturity point is expressed by n_t. We then compute a harmonic average of all the traded-weighted yields for a given maturity (Hwg).

3.3 The Extant Nelson-Siegel Model

The NS model is widely used in the practice of fitting term structure. The model for the forward rate curve is generally specified as:

$$f(\tau) = \begin{bmatrix}\beta_0\\ \beta_1\\ \beta_2\end{bmatrix}' \begin{bmatrix}1\\ e^{-\tau/\lambda}\\ (\tau/\lambda)e^{-\tau/\lambda}\end{bmatrix} = \begin{bmatrix}\beta_0\\ \beta_1\\ \beta_2\end{bmatrix}' \begin{bmatrix}f_0\\ f_1\\ f_2\end{bmatrix} \tag{3}$$

Where: τ is time to maturity, $\beta_0, \beta_1, \beta_2$ and λ are coefficients with λ > 0. The three factors are: f_0 a constant representing the (long-term) interest rate, f_1 an exponential decay function representing the slope of the curve, and f_2 a Laguerre function representing the curvature of the yield curve. The corresponding model for the spot rate curve is stated as:

$$r(\tau) = \begin{bmatrix}\beta_0\\ \beta_1\\ \beta_2\end{bmatrix}' \begin{bmatrix}1\\ \dfrac{\lambda\left(1-e^{-\frac{\tau}{\lambda}}\right)}{\tau}\\ \dfrac{\lambda\left(1-e^{-\frac{\tau}{\lambda}}\right)}{\tau} - e^{-\frac{\tau}{\lambda}}\end{bmatrix} = \begin{bmatrix}\beta_0\\ \beta_1\\ \beta_2\end{bmatrix}' \begin{bmatrix}r_0\\ r_1\\ r_2\end{bmatrix} \tag{4}$$

The three factors r_0, r_1, r_2 represent the level, slope and curvature of the spot rate curve. All other variables are as previously defined. Traditional parametric estimation methods for estimating the parameters of the NS model by either minimizing the SSE using OLS over a grid of pre-specified lambda values; or, using linear regression conditioned by a fixed shape parameter (Fabozzi et al. 2005).

3.3.1 Modeling NS by a Ridge Regression

Ridge regression is the most commonly used method to estimate the traditional three-factor NS model. Given a response vector $y \in \mathcal{R}^n$ and a predictor matrix $X \in \mathcal{R}^{n \times p}$, the ridge regression coefficients are defined as:

$$\widehat{\beta}^{ridge} = \frac{\text{argmin}}{\beta} \left(\sum_{i=1}^{n} (y_i - x_i'\beta)^2 + \lambda \sum_{j=1}^{p} \beta_j^2 \right) \tag{5}$$

Here $\lambda \geq 0$ controls the strength of the penalty term. Note that, when $\lambda = 0$ we get the linear regression estimate. Similarly when $\lambda = \infty$, we get $\widehat{\beta}^{ridge} = 0$. For λ in between, we are balancing two ideas: fitting a linear model of y *on* X, and shrinking the coefficients or penalizing the extreme observations. Essentially λ is the regularization constant. Ridge is the abbreviation for term structure yield curves produced by this technique.

3.3.2 Mapping NS using the K3-RANN

The K3-RANN is a single layer network that is known to offer excellent mapping capabilities. The K3-RANN has robust history in modeling financial data over several different time scales. For example, for hourly findings see Dash et. al. (2003) and Dash and Kajiji (2003); and, Dash and Kajiji (2008) for performance within the monthly domain. For performance comparisons across alternative ANN topologies, see Dash and Kajiji (2002). As with the generalized RANN method, the optimal weighting values, w_j, are generally extracted by applying a supervised least-squares method to a subset (training set) of the data series. The supervised learning function is stated as, $\boldsymbol{y} = f(\boldsymbol{x})$ where $\boldsymbol{y}$, the output vector, is a function of the input vector $\boldsymbol{x}$ with p number of inputs. The function can be restated as:

$$f(x_i) = \sum_{j=1}^{m} w_j h_j(x) \tag{6}$$

where, m is the number of basis functions (centers), h is the number of hidden units, w is the weight vector, and $i = 1..p$ where p is the number of input vectors. As shown by equation (7) the K3-RANN minimizes a modified SSE cost function:

$$\frac{\text{argmin}}{k} \left(\varsigma \sum_{i=1}^{p} (y - f(x_i \mid \bar{k}))^2 + \sum_{j=1}^{m} k_j w_j^2 \right) \tag{7}$$

The result of applying the K3-RANN is a set of weights (w_j) that minimize error (SSE) while optimizing the accuracy of the predicted fit (smoothness). The estimated weights are analogous to nonlinear least squares regression parameters. Hereafter, the estimated term structure curve generated by this technique is referred to as the K3-Hwg.

3.3.3 Modeling NS by the Support Vector Machine Regression

The support vector machine (SVM) is relatively new computing machine in the field of computational finance. The SVM algorithm is a nonlinear extension to the Generalized Portrait algorithm of Vapnick (1998). The SVR extension to the SVM learning algorithm is known to provide accurate, robust and very effective mapping across both small and large samples. When used as a regression mapping machine, given some training data X := $\{(x_1,y_1),\ldots,(x_l,y_l)\}$ drawn i.i.d. from some probability distribution P(x,y), the technique seeks to find a function f that minimizes the empirical risk function:

$$R_{emp}[f] = \frac{1}{l}\sum_{i=1}^{l} c\big(x_i, y_i, f(x_i)\big) \tag{8}$$

Estimating equation (8) directly could lead to overfitting and thus bad generalization especially if the training sample is small. Thus, a regularized risk functional is recommended:

$$R_{reg}[f] = \tfrac{1}{l}\textstyle\sum_{i=1}^{l} c\big(x_i, y_i, f(x_i)\big) + \tfrac{\lambda}{2}\|w\|^2 \ . \tag{9}$$

Here λ > 0 and is known as a regularization constant. This is similar to the regularization parameter k mentioned in the K3-RANN (equation (7)) and λ mentioned in ridge regression (equation (5)). The SVR extension formulated by Vapnik is:

$$\min\left[\frac{1}{2}\|w\|^2 + C\sum_{i=1}^{l}(\xi_i + \xi_i^*)\right] \tag{10}$$

$$\text{ST}\begin{cases} y_i - \langle w, x_i\rangle - b & \leq \quad \varepsilon + \xi_i \\ \langle w, x_i\rangle + b - y_i & \leq \quad \varepsilon + \xi_i^* \\ \qquad \xi_i, \xi_i^* & \geq \quad 0 \end{cases}$$

Where the constant C > 0 determines the trade-off between flatness of f and the amount up to which deviations larger than ϵ are tolerated. Term structure curves generated by this technique are labeled SVR.

A primary objective of this research is to identify which estimated term structure generates efficient curves in the presence of switching regimes. Computational similarities (e.g., regularization in the form of parameters λ and k) imply the more purposeful comparison of statistical difference in term structure curves involves the results generated by the K3-RANN and SVR methods.

4. Estimation Results

In this section we compare comparative results from mapping the term structure of trade yields.

4.1 The Municipal Market Regime Shift

The extensive bond yield literature reviewed previously described how switching-regime models are likely to describe historical yield rates better than single-regime models. Based on the observed time-series dispersion presented in section 2, a-priori we assume the possibility of a regime shift in municipal bond yields. In this section we search for the possibility of a two or more bond yield regimes by subjecting weighted average AAA YTW calculations to an SVM classification analysis. We start by following the arguments presented by Dai, et.al (2006). By assumption there are *S+1* “regimes” that govern the dynamic properties of the *N*-dimensional state vector *Y*. But, unlike the Dai (2006) formulation, the SVM mapping does not require the introduction of regime factor-variable. Still, in this machine learning approach agents are presumed to know the past histories of the state vector and the regime, but they are not required to recognize the regime the economy is in. Instead the Markov process governing regime changes is conditionally independent of the *Y* process. The result of mapping a 3-factor non-parametric SVM to YTM bond yields finds two regimes. As shown in figure 6 one regime is characterized by yields with bond maturities up to the 14-year maturity point on the AAA term structure. The transition to the second regime occurs between up to the 20-year spot.

<< Insert Figure 6 here >>

Although we are unable to generalize these findings across the investment grade credit spectrum, this initial finding adds new information about the regime switching behavior of municipal bond yields. The SVM results confirm earlier findings of how traditional single-regime factor-based modeling techniques are likely to understate yield fluctuations during the transition between regimes. We postulate that estimating the term structure using NS-inspired supervised learning networks will provide an effective alternative to ‘priced’ parametric factor models.

4.2 Time Series of 5, 10, 20 & 30 Year Spot for May, 2012

Figure 7A-D shows comparative term structure yields for 22 trading days in May-2012 at maturity points of 5, 10, 20 and 30 years. Model performance at the 5-year spot produced higher estimated yields than those reported by the subjectively constructed MMD benchmark. The relatively even estimation performance across models begins to dissipate at the 10-year spot and is completely eradicated at the 30-year spot. By observation, these results provide preliminary evidence that the alternate yield curves have a coherent estimation structure up to the 10-year maturity point. Conversely, for maturity periods greater than 10 years, yield curve mapping topology appears to have a significant bearing on the efficient pricing of traded municipal debt.

<< Insert Figures 7A - D here >>

4.3 Multiple Comparison Test

In this section we test the hypothesis of no relationship between the median of daily yields obtained from alternate models at a given maturity. Owing to a violation of the homogenous variance assumption, we apply the Mood's Median test – a special case of the Pearson Chi-Sq test (χ^2). Additionally, Cramer's V is used to identify the inter-correlation structure among the term-structure modeling results. We compute Cramer's V as follows:

$$\varphi_c = \sqrt{\frac{\chi^2}{N(k-1)}}\ where\ k = \min(R, C)\,; and\ N = Sample\ Size$$

We recognize that the Cramer's V is biased since it increases with the number of rows (R) of the contingency table or the number of columns (C) of the contingency table. In our case the rows are fixed at 2. Row 1 of the contingency table is the frequency count of all yields that are less than and equal to the median, and row 2 is the frequency count of all yields greater than the median. The columns in our contingency table are denoted by alternate computational methods. As observed from the above equation, the Cramer's V is related to the χ^2. When computed, we report only the Cramer's V statistic along with the asymptotic significance value (*p-value*). Because our goal is to identify where statistical differences among curve estimates are not statistically different, we bold the techniques that do not meet the significance test in tables 4, 5, 6, and 7.

4.3.1 5 Year Spot

The overall Median test indicates that there is a significant difference (χ^2 =76.772) between the median yields generated by the alternate computational techniques. Post hoc, Cramer's V is reported at 0.766; a finding leading us to conclude there is a relatively large effect (or differences) due to the application of alternate modeling techniques. Turning to table 4, it is revealed that the B-Spline term structure is not significantly different from the Ridge model (*p-value* = 0.150) or the SVR model (*p-value* = 0.172). Additionally, the ridge term structure is also not significantly different than K3-Hwg (*p-value* = 0.294). However, the K3-Hwg and B-Spline algorithmic methods are significantly different (*p-value* = 0.019). There is a very high effect size with Ridge, K3-Hwg, and B-Spline (each produces a Cramer's V > 0.70).

Table 4. Cramer's V for the 5-yr Spot

	Ridge	SVR	K3-Hwg	B-Spline
MMD	0.872	0.563	0.956	0.719
	(0.000)	(0.000)	(0.000)	(0.000)
Ridge		0.413	**0.158**	**0.217**
		(0.007)	**(0.294)**	**(0.150)**
SVR			0.533	**0.208**
			(0.000)	**(0.172)**
K3-Hwg				0.354
				(0.019)

Note: *p-values* of the Craver's V are in parenthesis

4.3.2 10 Year Spot

Table 5 presents the post hoc results for the overall Median test. The results provide evidence that there is a significant difference (χ^2 =59.638) between the median yields generated by the alternate modelling methodologies. Cramer's V effect size is 0.672; a finding which indicates a relatively large effect due to the application of alternate models. While significantly different than the SVR model results, the post-hoc analysis (table 5) reveals K3-Hwg is not significantly different from the Ridge model. As previously reported, the MMD yields remain significantly different than all computation techniques.

Table 5. Cramer's V for the 10-yr Spot

	Ridge	SVR	K3-Hwg	B-Spline
MMD	0.577	0.832	0.542	1.000
	(0.000)	(0.000)	(0.000)	(0.000)
Ridge		0.336	**0.046**	0.577
		(0.026)	**(0.763)**	(0.000)
SVR			0.378	0.316
			(0.012)	(0.036)
K3-Hwg				0.612
				(0.000)

Note: *p-values* of the Cramer's V are in parenthesis

4.3.3 20 Year Spot

The overall Median test results indicate that there is a significant difference (χ^2 =24.364) between the median yields generated by the alternate models. Cramer's V total effect size is 0.471; a level that suggest a moderate effect (or differences) attributable to alternate model application. The post hoc analysis is presented in table 6. At the 20-yr spot the alternate models estimate significantly different yields than those reported by the subjectively computed benchmark MMD term structure. Both SVR with B-Spline, and K3-Hwg with Ridge report small effect sizes.

Table 6. Cramer's V for the 20Yr Spot

	Ridge	SVR	K3-Hwg	B-Spline
MMD	0.688 (0.000)	0.408 (0.007)	0.607 (0.000)	0.448 (0.003)
Ridge		0.327 (0.030)	**0.102 (0.498)**	**0.283 (0.060)**
SVR			**0.229 (0.128)**	**0.046 (0.763)**
K3-Hwg				**0.185 (0.220)**

Note: *p-values* of the Craver's V are in parenthesis

4.3.4 30 Year Spot

As with the 30-yr spot, the result of applying the overall Median test indicates a significant difference (χ^2 =31.273) among the median yields generated by the alternate models. The total effect size from Cramer's V is 0.487. As with the 20-year spot, there is only a moderate effect attributable to the alternate models. Table 7 reports the post hoc analysis. In a manner that is consistent with all other spots, the MMD yield is significantly different from all other computed yields. The smallest effect size is captured between Ridge with K3-Hwg. B-Spline measured against both Ridge and K3-Hwg follows close behind. The SVR technique reports the largest difference in effect size measured against Ridge and K3-Hwg.

Table 7. Cramer's V for the 30yr Spot

	Ridge	SVR	K3-Hwg	B-Spline
MMD	0.719 (0.000)	0.542 (0.000)	0.756 (0.000)	0.683 (0.000)
Ridge		**0.229 (0.128)**	**0.050 (0.741)**	**0.048 (0.750)**
SVR			**0.277 (0.066)**	**0.183 (0.226)**
K3-Hwg				**0.098 (0.517)**

Note: p-values of the Cramer's V are in parenthesis

4.3.5 Modeling Summary

By way of section summary, when we deployed alternate models to map the U.S. municipal bond term structure the results showed that Ridge and K3-Hwg do not produce significantly different estimates of YTW. This is not completely surprising as the K3-Hwg mapping embodies a modified ridge regression. Correspondingly, at only one spot (30-year) was Ridge compared to SVR not significantly different. At the 5% level, Ridge and B-Spline are not significantly different at the 5-, 20-, and 30-year spots. At $p \leq 0.10$ Ridge and B-Spline are significantly different at the 20-year spot. The research interests of this research are directed pointedly at the performance of the SVR and K3-Hwg models. Interestingly, these two methods are not significantly different at the 20- and 30-year spots; sport on the term structure that occurs after the transition to a different regime. Lastly, as reported in table 8, for May-2012 the K3-Hwg model produced the lowest comparative RMSE at tested points across the term structure.

Table 8. RMSE for the spot rates

	Ridge	**SVR**	**K3-HWg**
5Yr	0.01137	0.01134	0.00110
10Yr	0.01882	0.01866	0.00138
20Yr	0.02602	0.02602	0.00456
30Yr	0.02889	0.02892	0.00698

As reported in the literature, spline and ridge techniques provides accurate estimates of bond yields in a single-regime economy. However, based on the performance results provided herein, like previously reported findings these non-mapping methods produce unstable and estimates post regime transition. With evidence of a regime transition period around the 14-year maturity, both K3-Hwg and SVR produce homogenous yield estimates post transition (20- and 30-year spots). In summary, while closely related to the performance of the SVR, the K3-Hwg model matched the modeling results of the single-regime Ridge model. Post regime switch, the K3-Hwg model results were confirmed by near identical results from solving the SVR model. Overall, the K3-Hwg model is the preferred method for mapping dynamic bond yield term structure with the expectation for regime-shift risks.

5. The Production of Traded Bond Liquidity and Factor Scale-Elasticity

This section of the paper proposes a RANN methodology to generalize the returns-to-scale of individual municipal bond liquidity using bond characteristics and macroeconomic data as production factor proxies. Comparative scale effects are estimated using both parametric and nonparametric methods. We begin by describing the importance of bond liquidity. This is followed by a description of the bond generalized bond production function. Lastly, we introduce the alternative modeling methodologies.

5.1 Bond Illiquidity

The research strain investigating transaction costs, liquidity, and creditworthiness reports lower creditworthiness is associated with higher transactions costs. To the extent that transaction costs influence the willingness of counterparties to conduct a trade this finding implies there may be an impact on bond liquidity (see for example, Edwards, Harris and Piwowar (2007)). Earlier, Harris and Piwowar (2006) reported how municipal bond trading costs increase with time to maturity and bond complexity. Importantly, they found lower and negligible differences in trading costs among investment grade bonds rated AA and above. In an investigation of trade size, Edwards, Harris and Piwowar (2007) also reported how recently issued bonds and bonds closer to maturity produce lower trade costs. This study also finds a positive relationship between creditworthiness and transactions costs. Bao, Pan and Wang (2011) shifted the study of illiquidity to yield spread components. They were unable to show that a given illiquidity measure produces a significant relationship between creditworthiness and bond liquidity. In study of how dealers' manage illiquid assets within a 30-day window of purchase, Goldstein and Hotchkiss (2015) report that dealers act more like brokers as they manage holding period risk more aggressively for less liquid bonds. However, they do not report a significant relationship between their measure of transaction costs (dealer roundtrip spreads) and investment grade bonds.

The literature provides evidence that increased liquidity and lower (stable) transactions cost influences efficient pricing in bond markets. We propose a methodology to estimate generalized bond liquidity from traded instruments. The model's proxies for liquidity response variables are three well-known liquidity measures: Amihud (Ami), IRC and the modified IRC (IRCm). Details are provided next.

5.1.1 Amihud

The daily Amihud (2002) measure is calculated as the average ratio of absolute return to the trade size of consecutive transactions during a day:

$$Amihud_{i,t} = \frac{1}{N_{i,t}} \sum_{j=1}^{N_{i,t}} \frac{\left| \frac{P_{i,j} - P_{i,j-1}}{P_{i,j-1}} \right|}{Q_{i,j}} \tag{11}$$

5.1.2 IRC

The Feldhütter (2012) imputed round-trip cost, IRC, takes into consideration the dispersion of traded prices around the market-wide consensus bond valuation:

$$IRC_{i,t} = \frac{p_{i,t}^{\max} - p_{i,t}^{\min}}{p_{i,t}^{\min}} \tag{12}$$

Here, P^{max} is the largest price in an imputed round trip and P^{min} is the smallest. On a given day, when several trades occur on a given bond with the same trade size the measure assumes the trades reflect the dealer imposed bid-ask spread and reflect a dealer taking one side of a trade only to offset the trade at a later point in the day.

5.1.3 Modified IRC

The modified imputed roundtrip cost (IRCm) treats a round trip as a transaction between a dealer and customer; a dealer to a different dealer; or, a trade between two customers.

To examine the production of generalized bond liquidity we shift the analysis to a monthly time series. In the month of February, 2014 the three liquidity measures are calculated for each traded bond.

5.2 The Parametric Double-Log Production Function

The double log (Cobb and Douglas 1928) functional form of the production function is well known for its representation of the functional relationship of an output to factor inputs. A popular form of the double-log model is the well-known Cobb-Douglas function. For our purposes, the generalized double-log model is expressed as:

$$f(x) = A\prod_{i=1}^{n} x_i^{\beta_i}, \beta_i > 0, i = 1, 2, \ldots n \tag{13}$$

This functional form has the following properties: a) Strict monotonic – if x'> x then *f(x') > f(x)*; b) Quasi-concavity – $V(y) = [x : f(x) \geq y]$ is a convex set; c) Strict essentiality – $f(x_a, \ldots x_{i-1}, 0, x_{i+a}, \ldots, x_n) = 0$ for all $x_i > 0$; d) the set *V(y)* is finite, nonnegative, real valued and single valued for all nonnegative and finite *x*. It is also continuous and everywhere twice-continuously differentiable; e) *f(x)* is homogenous of degree *k* = sum of β_I. Additionally, stated in this functional form all inputs can be interchanged without affecting output and each input must be used in strictly positive amounts to obtain a positive output. Where necessary, transformation to the zero-value arguments is applied. Despite imposing a unit elasticity of substitution the simple double-log specification has proven useful and accurate in a study by Juillard and Villemot (2011) on real business cycles. Extant literature does not express a preference for any one particular liquidity proxy; hence, we propose an economic model to jointly estimate the elasticity of municipal bond liquidity by utilizing three liquidity response variables: Amihud, IRC, and IRCm. The model is formally stated as:

$$Ln(Y_{A,R,I}) = LnA + \sum_{i=1}^{n} \beta_i Ln(x_i) + \varepsilon, \tag{14}$$

where $\beta_i = 1, 2, \ldots, n$ and $\epsilon \sim N(0,1)$. Components of ***Y*** include the Amihud (A), IRC (R), and modified IRC (I) liquidity measures. Predictor variable proxies, x_i, are identified in table 9.

Table 9. Predictor variables used for modelling the illiquidity

Variable	**Information Effect Factor**	**Source**
Abs Diff of YTWs (AbsDifYTW)	Instrument	YTW spread vs K3
Days to Maturity	Instrument	MSRB
Trade Size	Market	MSRB
Trade Price	Market	MSRB
State Building Permits (Bldg Permits)	Macroeconomic	US Census Bureau
State Civilian Labor Force (Labor)	Macroeconomic	US Census Bureau
Convexity	Instrument risk	Computed

5.3 RTS implications

Scale economies are a measurement of the amount bond liquidity (output) changes if all liquidity input factors (bond and macroeconomic factors) change by the same amount. In the decision-making process, bond scale economies provide insight into pricing policies, market structure and, government intervention or regulation. The investigation in this section of the paper involves the largely unexplored nature of estimating generalized bond returns-to-scale (RTS) by alternative approaches and then reconciling computational differences to enumerate probable scale economics. We follow the arguments of Kajiji and Dash (2013) by comparing parameter estimates obtained by mapping the multivariate K7-RANN against estimates from a multivariate GLS (SPSS v23). For the month of Feb-2014, tables 10-14 present the weekly estimated elasticity coefficients for both models. The weekly RTS is the sum of the input elasticities.

Table 10. Week 1 parameter estimates illiquidity measure using alternate techniques.

	MRANN			Multivariate Regression		
Predictors\Targets	Amihud	IRC	IRCm	Amihud	IRC	IRCm
Ln(AbsDiffYTW)	0.064	0.524	0.425	0.096*	0.047	0.069
Ln(Trade Size)	0.734	0.314	0.293	-0.026	0.064	0.078
Ln(Trade Price)	-1.142	-0.848	-0.969	-1.750*	-4.014*	-3.932*
Ln(Days To Maturity)	1.899	1.413	1.522	-0.319*	0.499*	0.403*
Ln(Bldg Permits)	-0.970	-0.702	-0.623	-0.871*	-0.677*	-0.681*
Ln(Labor)	-1.076	-0.623	-0.748	1.001*	0.951*	0.966
Ln(Convexity)	1.402	0.622	0.79	0.008	-0.038	-0.029
RTS Week 1 N=6161	1.319	1.234	1.366	-0.018	0.073	1.084

Note: $*p < 0.05$.

Table 11. Week 2 parameter estimates illiquidity measure using alternate techniques.

	MRANN			Multivariate Regression		
Predictors\Targets	Amihud	IRC	IRCm	Amihud	IRC	IRCm
Ln(AbsDiffYTW)	37.135	19.323	18.342	0.079	0.169*	0.183*
Ln(Trade Size)	5.321	3.291	3.277	0.058	0.120*	0.115*
Ln(Trade Price)	1.635	0.172	-0.204	-2.319*	-3.684*	-3.644*
Ln(Days To Maturity)	-35.606	-17.151	-15.705	-0.178	0.476*	0.458*
Ln(Bldg Permits)	3.299	2.263	2.383	-0.963*	-0.552*	-0.536*
Ln(Labor)	0.774	0.254	0.234	1.081*	0.763*	0.754*
Ln(Convexity)	-9.539	-6.154	-6.322	0.007	-0.048*	-0.053*
RTS Week 2 N=5670	3.019	1.998	2.005	-0.034	0.000	0.000

Note: $*p < 0.05$.

Table 12. Week 3 parameter estimates illiquidity measure using alternate techniques.

	MRANN			Multivariate Regression		
Predictors\Targets	Amihud	IRC	IRCm	Amihud	IRC	IRCm
Ln(AbsDiffYTW)	1.338	1.022	1.077	-0.040	-0.028	-0.028
Ln(Trade Size)	3.619	3.308	3.437	-1.737	0.198*	0.207*
Ln(Trade Price)	-4.065	-3.801	-3.994	-0.193*	-3.064*	-3.084*
Ln(Days To Maturity)	-5.028	-4.350	-4.468	-0.833	0.257	0.279
Ln(Bldg Permits)	6.831	5.865	6.138	0.868*	-0.580*	-0.568*
Ln(Labor)	-2.768	-2.742	-2.981	-1.737*	0.655*	0.634*
Ln(Convexity)	1.446	1.646	1.760	0.032	-0.005	-0.010
RTS Week 3 N=4722	1.373	0.948	0.969	-2.578	0.224	0.241

Note: $*p < 0.05$.

Table 13. Week 4 parameter estimates illiquidity measure using alternate techniques.

	MRANN			Multivariate Regression		
Predictors\Targets	Amihud	IRC	IRCm	Amihud	IRC	IRCm
Ln(AbsDiffYTW)	-0.044	0.004	-0.039	0.013	-0.001	0.028
Ln(Trade Size)	1.192	0.467	0.441	0.049	0.148*	0.155*
Ln(Trade Price)	0.617	0.333	0.358	-1.654*	-3.182*	-3.141*
Ln(Days To Maturity)	0.063	0.383	0.374	0.010	0.300*	0.212*
Ln(Bldg Permits)	-0.674	-0.416	-0.380	-1.109*	-0.907*	-0.939*
Ln(Labor)	-0.143	0.040	0.047	0.867*	0.857*	0.901
Ln(Convexity)	0.716	0.343	0.368	-0.025	-0.036	-0.026
RTS Week 4 N=5811	1.727	1.154	1.169	0.047	-0.037	0.903

Note: $*p < 0.05$.

The analysis of these four tables begins with a review of weekly RTS. Except for week 3, all weekly K7-MRANN RTS estimates exhibit increasing returns to scale (IRS). The IRS finding suggests that at an economic decision point bond liquidity experiences a greater percentage change than the simultaneous changes realized by all input variables. For example, take week 4. The Amihud RTS implies that the bond's Amihud liquidity measure will increase by 1.727 percent for a one-percent simultaneous change in the factor inputs. Only in week 3 and according to the values for IRC and IRCm is the reported RTS diminishing (but close to unity, or constant RTS).

The multivariate GLS results do not produce uniform RTS results across the weeks of the month. In fact, for many months the Amihud RTS is negative or zero. We do not provide further analysis of the GLS scale elasticities as the results lack consistency with historical findings and beg for an interpretation that would shed new light on evolving a descriptive theory for the efficient trading of municipal bonds. Instead, we devote the remainder of this section to an in-depth analysis of the variable scale elasticities generated by the K7-MRANN mapping.

5.3.1 YTW Spread vs K3

Previously we noted that Bao, Pan and Wang (2011) reported illiquidity was a substantial component of spread rates. Their study was unable to confirm a significant relationship between the credit rating of IG bonds and liquidity. To capture this effect, we include the proxy factor computed as the absolute value of the spread between the traded bond's YTW and the K3-Hwg efficient yield. This particular spread calculation captures overall pricing inefficiency for the traded bond. Except for week 4 where IRC deviates, in each week the factor elasticity across each liquidity domain bears the same sign. Mostly positive across the month, this elasticity suggests that as the spread between actual bond yield and the K3-Hwg benchmark widen, bond liquidity increases.

5.3.2 Days to Maturity

By reflection we noted the Harris and Piwowar (2006) study reported bond trading costs increase (i.e., illiquidity increases) with instrument time to maturity (complexity and age). The elasticity metrics for this variable are interesting as they differ by week. All three liquidity proxies have positive elasticity values in weeks 1 and 4. Amihud is reported at 1.899 and 0.062, respectively. We also note week 2 reports the lowest number of bond trades. The two middle weeks of the month display consistently negative elasticities with a correspondingly low number of bond trades. The reported elasticity values for these two weeks are -35.606 and -5.028, respectively. To the decision-maker this implies the need for a weekly analysis of scale economies along with an analysis of the type of trades (clients) within week.

5.3.3 Trade Size

Edwards, Harris and Piwowar (2007) examined the impact of trade size on transactions costs and liquidity. The study found trade size and transaction costs move inversely thereby implying increased liquidity. Trade size decline is often associated with an increase in retail participation. A recent FINRA analysis notes that price impacts associated with the size of a trade are, on average, transitory and is not necessarily indicative of dealer profitability in block trades (Mizrach 2015). The trade size elasticity metrics are completely uniformly positive across measures and weeks. This finding complements earlier findings on the relation to transactions costs. In this study, we find bond liquidity increases as trade size increase.

5.3.4 Trade Price

Edwards, Harris and Piwowar (2007) also showed that bonds with transparent trade prices have lower transactions costs; a finding that supports the expectation of increased market liquidity. Based on the computed Amihud value, trade price elasticity (i.e., absolute value) is elastic in weeks 1 (-1.142), 2 (1.635), and 3 (-4.065). In weed 4 trade price elasticity is consistently represented as inelastic (e.g., 0.617). The liquidity reaction to a change in price ranges from a low of 0.617 percent to a high of 4.065 percent.

5.3.5 State Building Permits and State Civilian Labor Force

Earlier we reviewed confirmatory evidence of improved yield predictions from the addition of macroeconomic factors to the base NS model. State building permits have a direct impact on related economic activities such as financing and employment. The state civilian labor force measure captures all employed persons as well as the unemployed who are actively seeking employment. Variation in this rate is an indicator of overall economic activity. Using the Amihud result, in week 1 both factor coefficients are negative (uniformly, as economic activity increases bond liquidity declines). In week 2 both are positive (uniformly, as economic activity increased bond liquidity increases). In week 3 the decision-maker must evaluate each proxy separately as the coefficient for building is positive while the labor coefficient is negative. By week 4 both factors coefficients have a negative sign attached. Clearly, the source of macroeconomic activity is important to determining changes to bond liquidity.

5.3.6 Risk Factor Convexity

We capture nonlinear changes in bond price relative to yield changes by including bond convexity. Convexity is a measure of the curvature of the changes in bond price in relation to changes in yields. The Amihud convexity findings are positive except in week 2. Positive convexity is known to increase bond return. For example, in week 2 convexity elasticity is reported as 1.446 implying a one-percent increase in convexity will result in a 1.446 percent increase in bond liquidity.

5.3.7 The Municipal Bond Decision Process for Efficient Trades

As reasoned in this research, the decision theoretic process for trading municipal bonds in the U.S. municipal bond market involves the execution of six distinct steps. The first step is to "Decide to trade". The second step is to obtain MSRB near-real time trade information. The third step is to cull and munge the Big Data on the MSRB tape. Fourth, step is to update the NS daily term structure curve using the K3-RANN; or, secondarily, SVR. The fifth step is to up-date the weekly bond-trading liquidity valuation model. The sixth and final step is to compute production RTS with a factor greater than unity indicating a feasible weekly environment in which to trade s specific bond at the K3-Hwg equilibrium price.

6. Summary and Conclusions

This paper was motivated from concerns expressed by regulators and market participants alike about the lack of transparency in secondary market operation across the U.S. municipal bond market. This concern incorporates the inability of the industry to establish a set of benchmark yield curves across all investment level credit grades. As such, a primary objective of this paper sought to establish a decision-processes required to design an optimal municipal bond trading policy. After providing an institutional view of trades reported on the MSRB trade tape, the research turned to the development of a new benchmark term structure. The big data characteristics of the MSRB trade tape encouraged this initial investigation to sample within credit ratings and by time period. Using all trades for AAA rated bonds we invoked artificial intelligence mapping to develop alternate yield curves for statistical evaluation and comparison. Prior to producing a multiple comparison examination the research also addressed switching regimes in the AAA term structure. Using SVM analytics, a regime shift was detected at approximately the 14-year spot with the transition to the next regime fully accomplished by the 20-year spot. With a focus on curves generated by ridge regression, a K3-RANN, and a SVR we provided MSE-based evidence that the NS K3-Hwg produced statistically superior term structure within the switching regime environment.

We synthesize our empirical findings by multivariate mapping of a production-theoretic RTS derived from traded municipal bonds. As part of this process, we use the estimated factor elasticity metrics to support the implementation of a weekly bond trade policy relative to changes in individual bond liquidity. Lastly, we find a production relationship between liquidity production and macroeconomic factor conditions. Premised by the weekly RTS this research demonstrates the importance of both daily and weekly valuation updates.

With MSRB data now fully distributed, future research will certainly want to investigate bond liquidity and valuation decisions in greater detail. In addition to cross-sectional views, credit differentiated yield curves and their relationship to bond liquidity are sure to mimic similar studies directed at the corporate bond markets. However, in the case of the municipal market, there is a chance to take valuation studies a step further by relating new yield curves to sectors and Federal Reserve districts.

References

Aguilar LA (2015) Statement on Making the Municipal Securities Market More Transparent, Liquid, and Fair U.S. Securities and Exchange Commission, http://bit.ly/2uOsamN

Almeida C, Kubudi D, Simonsen AA, Vicente J (2013) Forecasting Bond Yields with Segmented Term Structure Models.

Amihud Y (2002) Illiquidity and Stock Returns: Cross-Section and Time-Series Effects Journal of Financial Markets 5:pp 31-56

Ang A, Piazzesi M (2003) A No-Arbitrage Vector Autoregression of Term Structure Dynamics with Macroeconomic and Latent Variables Journal of Monetary Economics 50:745-787

Annaert J, Claes AGP, De Ceuster MJK, Zhang H Estimating the Yield Curve Using the Nelson-Siegel Model. In: European Financial Management Association Aarhus, Denmark, 2010.

Bao J, Pan J, Wang J (2011) The illiquidity of Corporate Bonds The Journal of Finance 66:911-946

Bowsher CG, Meeks R (2013) Stationarity and the Term Structure of Interest Rates: A Characterization of Stationary and Unit Root Yield Curves.

Cobb CW, Douglas PH (1928) A Theory of Production American Economic Review 18:139-165

Cox JC, Ingersoll JE, Ross SA (1985) A Theory of the Term Structure of Interest Rates Econometrica 53:385-408

Creal DD, Wu CJ (2014) Estimation of Affine Term Structure Models with Spanned or Unspanned Stochastic Volatility.

Dai Q, Singleton KJ (2000) Specification Analysis of Affine Term Structure Models Journal of Finance 55:1943-1978

Dai Q, Singleton KJ, Yang W (2007) Regime Shifts in a Dynamic Term Structure Model of U.S. Treasury Bond Yields Review of Financial Studies, Society for Financial Studies 20:1669-1706

Daniels K, Ejara DD (2009) Impact of Information Asymmetry on Municipal Bond Yields: An Empirical Analysis American Journal of Economics and Business Administration 1:11-20

Dash Jr. GH, Hanumara C, Kajiji N Neural Network Architectures for Modeling FX Futures Options Volatility. In: Annual Meetings of the Northeast Decision Sciences Institute, Providence, Rhode Island, 2003.

Dash Jr. GH, Kajiji N Modeling FX Volatility: A Comparative Analysis of the RBF Neural Network Topology. In: 9th International Conference on Forecasting Financial Markets, London, England, 2002.

Dash Jr. GH, Kajiji N (2003) New Evidence on the Predictability of South African FX Volatility in Heterogenous Bilateral Markets The African Finance Journal 5:1-15

Dash Jr. GH, Kajiji N (2008) Engineering a Generalized Neural Network Mapping of Volatility Spillovers in European Government Bond Markets. In: Zopounidis C, Doumpos M, Pardalos PM (eds) Handbook of Financial Engineering, vol 18. Optimization and Its Applications. Springer,

De Pooter M (2007) Examining the Nelson-Siegel Class of Term Structure Models. Tinbergen Institute, The Netherlands

De Pooter M, Ravazzolo F, van Dijk DJC (2010) Term Structure Forecasting Using Macro Factors and Forecast Combination.

Diebold FX, Li C (2006) Forecasting the Term Structure of Government Bond Yields Journal of Econometrics 130:337-364

Diebold FX, Rudebusch GD, Boragan AS (2006) The Macroeconomy and the Yield Curve: A Dynamic Latent Factor Approach Journal of Econometrics 131:309-338

Edwards AK, Harris LE, Piwowar MS (2007) Corporate bond market transaction costs and transparency Journal of Finance 62:1421-1451

Fabozzi FJ, Martellini L, Priaulet P (2005) Predictability in the Shape of the Term Structure of Interest Rates Journal of Fixed Income 15:40-53

Feldhütter P (2012) The Same Bond at Different Prices: Identifying Search Frictions and Selling Pressures Review of Financial Studies 25:1155-1206

Goldstein M, Hotchkiss ES (2015) Dealer Behavior in Highly Illiquid Risky Assets. Queens University, Belfast, UK

Gonzalez-Rozada M, Sola M, Hevia C, Spagnolo F (2012) Estimating and Forecasting the Yield Curve Using a Markov Switching Dynamic Nelson and Siegel Model. Universidad Torcuato Di Tella,

Harris LE, Piwowar MS (2006) Secondary Trading Costs in the Municipal Bond Market Journal of Finance 61:1361-1397

Iglewicz B, Hoaglin D (1993) Volume 16: How to Detect and Handle Outliers. In: Mykytka EF (ed) The ASQC Basic Reference in Quality Control: Statistical Techniques.

Juillard M, Villemot S (2011) Multi-Country Real Business Cycle Models: Accuracy Tests and Test Bench Journal of Economic Dynamic and Control 35:178-185

Kajiji N (2001) Adaptation of Alternative Closed Form Regularization Parameters with Prior Information to the Radial Basis Function Neural Network for High Frequency Financial Time Series. University of Rhode Island

Kajiji N, Dash Jr. GH (2013) On the Behavioral Specification and Multivariate Neural Network Estimation of Cognitive Scale Economies Journal of Applied Operational Research 5

Kalotay AJ, Dorigan M (2008) What makes the Municipal Yield Curve Rise? The Journal of Fixed Income Winter

Lin H, Liu S, Wang J, Wu C Liquidity and the Pricing of Municipal Bonds. In: Proceedings of the 2010 China International Conference in Finance, Beijing, China, 2010.

Mizrach B (2015) Analysis of Corporate Bond Liquidity. FINRA Office of the Chief Economist, http://bit.ly/2wbO9Dw

Moench E (2008) Forecasting the Yield Curve in a Data-Rich Environment: A No-Arbitrage Factor-Augmented VAR Approach Journal of Econometrics 146

Nelson CR, Siegel A (1987) Parismoious Modeling of Yield Curves Journal of Business 60:473-489

Olej V, Hájek P (2009) Municipal Creditworthiness Modelling by Radial Basis Function Neural Networks and Sensitive Analysis of their Input Parameters. In: Alippi C, Polycarpou M, Panayiotou C, Ellinas G (eds) Artificial Neural Networks - ICANN 2009. Lecture Notes in Computer Science. Springer Berlin Heidelberg, pp 505-514

Steenbarger BN (2003) The Psychology of Trading: Tools and Techniques for Minding the Markets. John Wiley & Sons, NJ

Vapnik V (1998) Statistical Learning Theory. Wiley-Interscience, New York

Vasicek O (1977) An Equilibrium Characterization of the Term Structure Journal of Financial Economics 5:177-188

Xiang J, Zhu X (2013) A Regime-Switching Nelson-Siegel Term Structure Model and Interest Rate Forecasts Journal of Financial Econometrics 11:522-555

Figure Captions

Fig. 1 Participants traders of investment grade bonds

Fig. 2 Daily dispersion of AAA trades for May-2012

Fig. 3 Daily dispersion of AAA trades for February-2014

Fig. 4 Daily AAA term structure for May, 2012

Fig. 5 Daily AAA term structure for Feb, 2014

Fig. 6 SVM regime shift identification (May 1, 2012)

Fig. 7A May-2012 alternative term structure at the 5-year spot

Fig. 7B May-2012 alternative term structure at the 10-year spot

Fig. 7C May-2012 alternative term structure at the 20-year spot

Fig. 7D May-2012 alternative term structure at the 30-year spot

Figure 1 Click here to download Figure Fig1.png

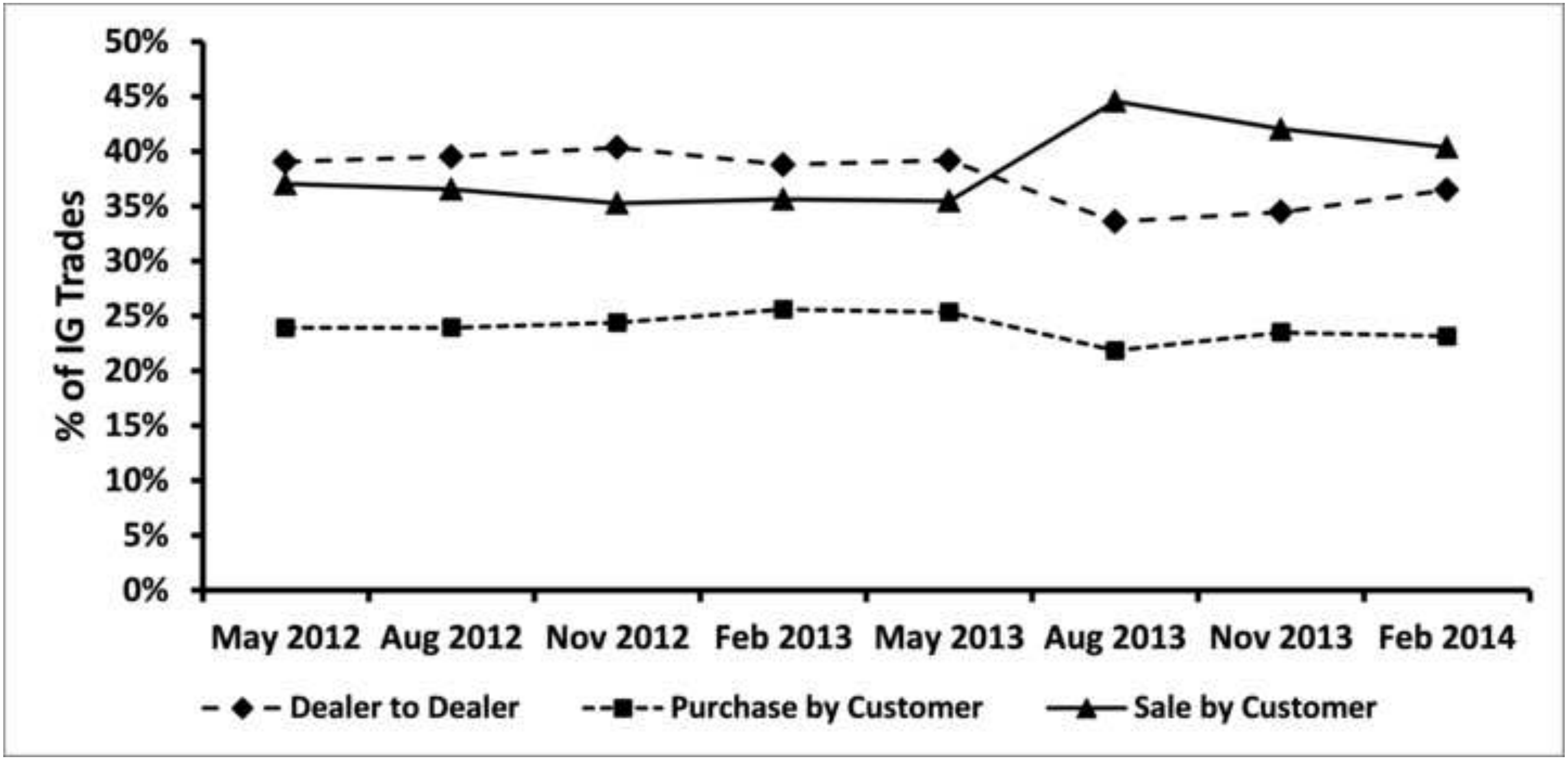

Figure 2

Click here to download Figure Fig2.png

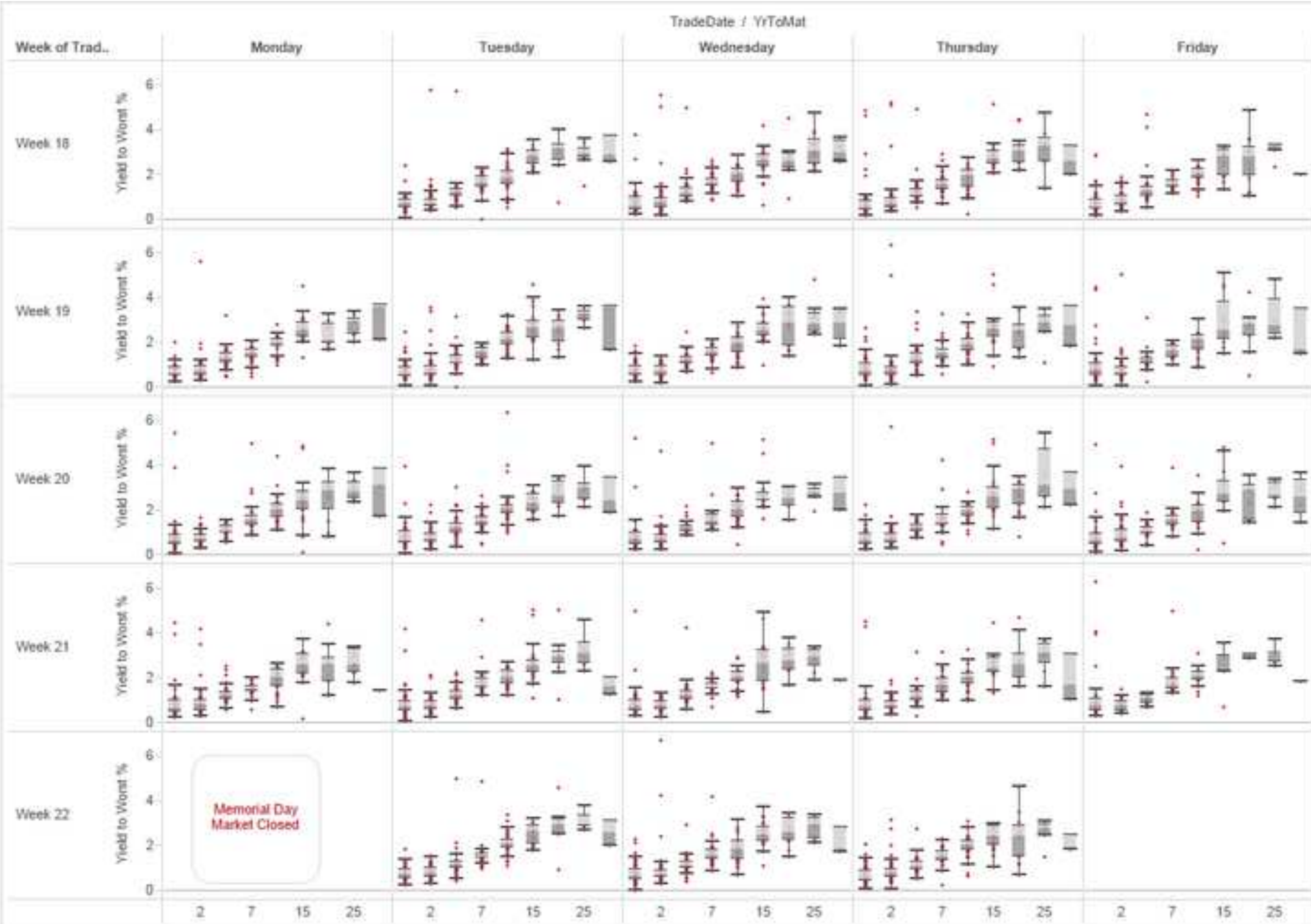

Figure 3 Click here to download Figure Fig3.png

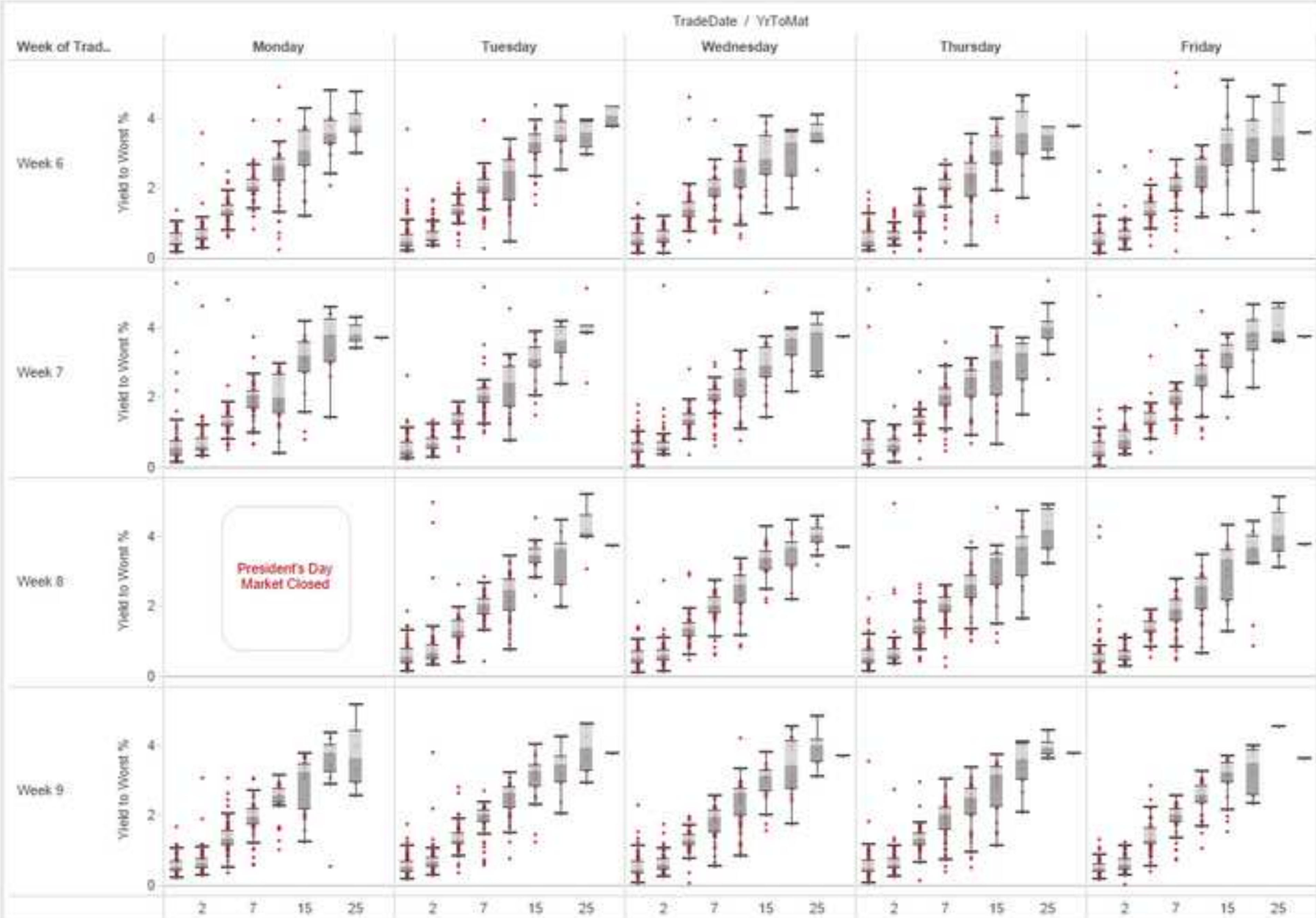

Figure 4

Click here to download Figure Fig4.png

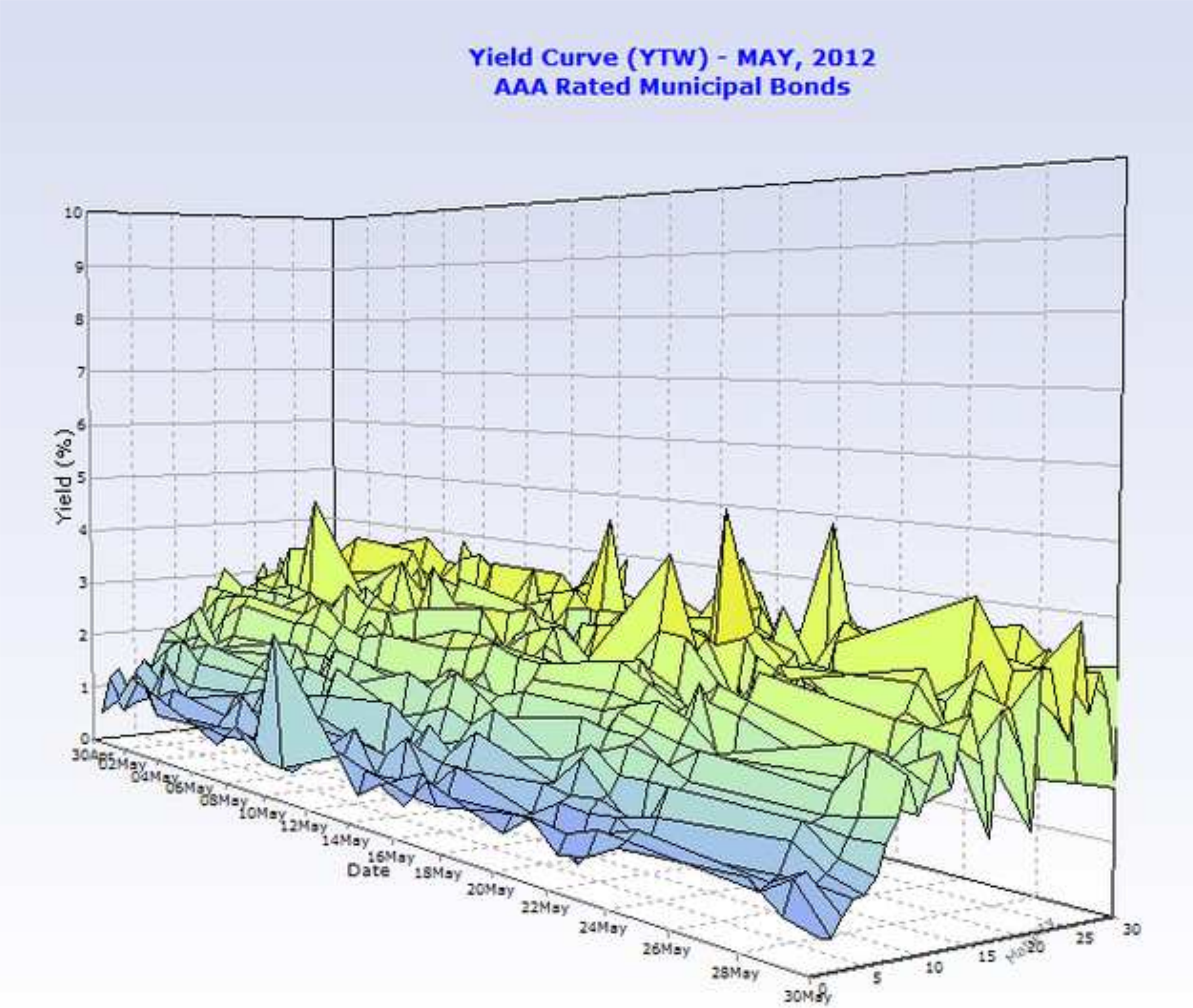

Figure 5

Click here to download Figure Fig5.png

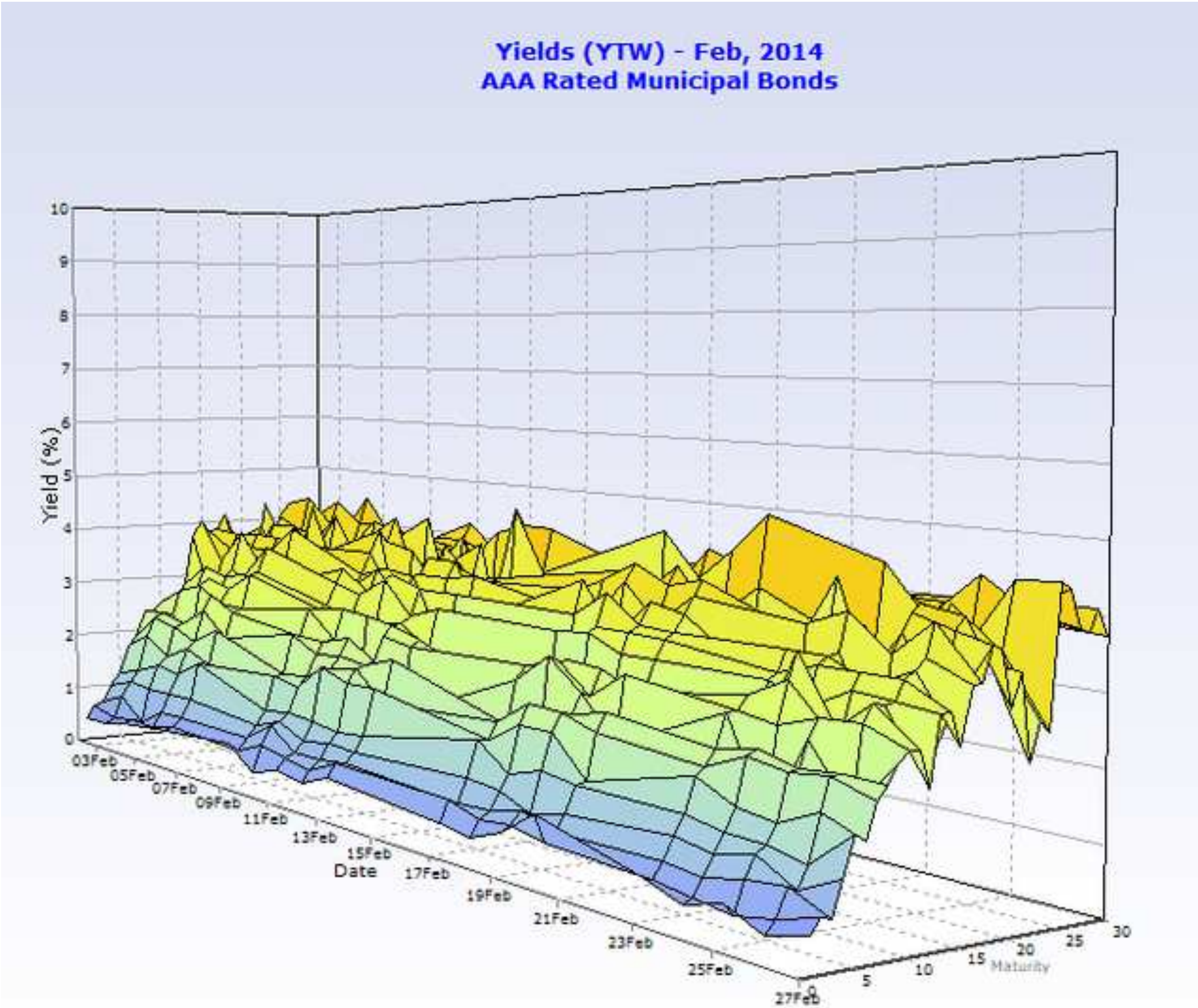

Figure 6 Click here to download Figure Fig6.png

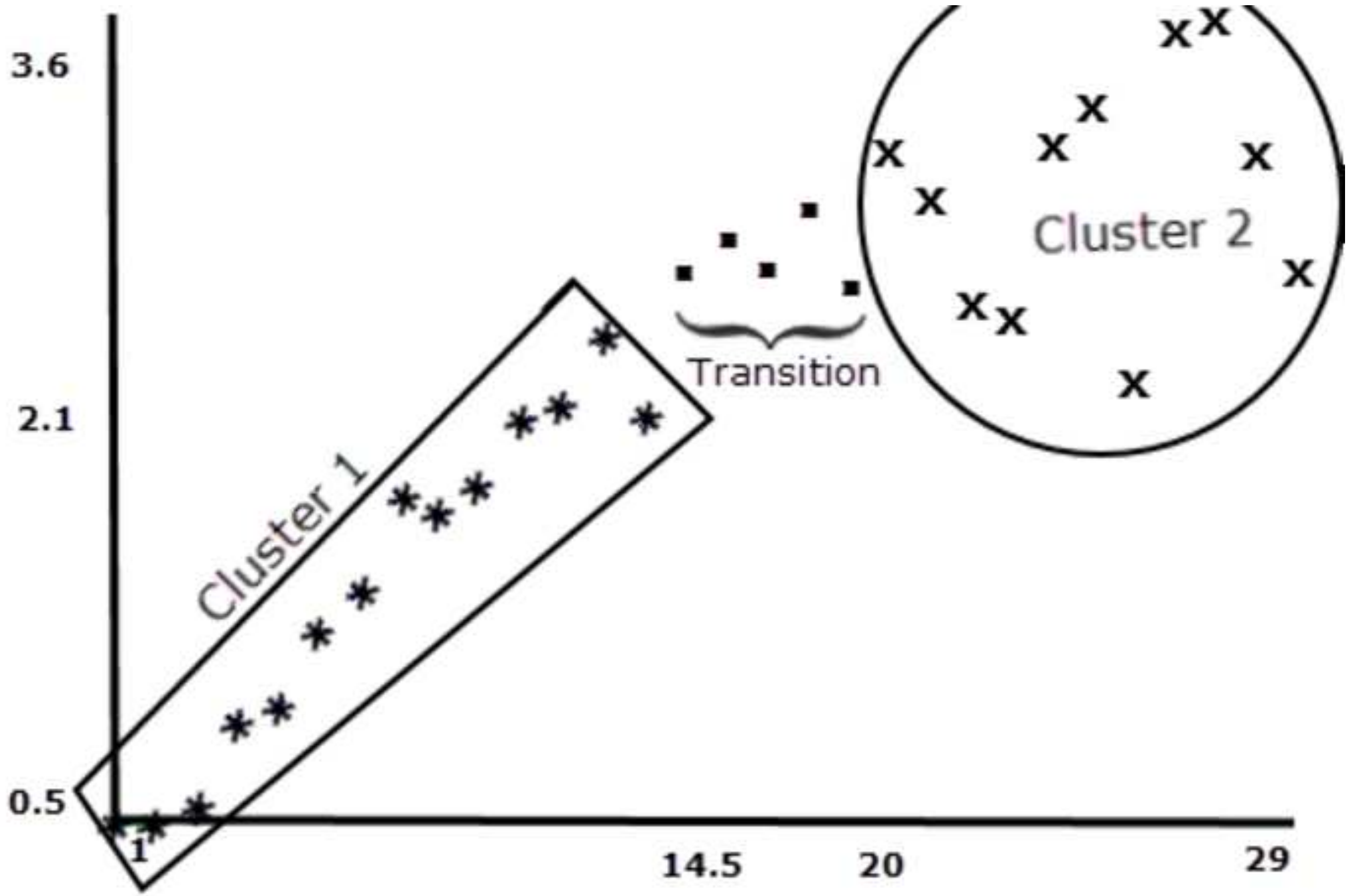

Figure 7A

Click here to download Figure Fig7A.png

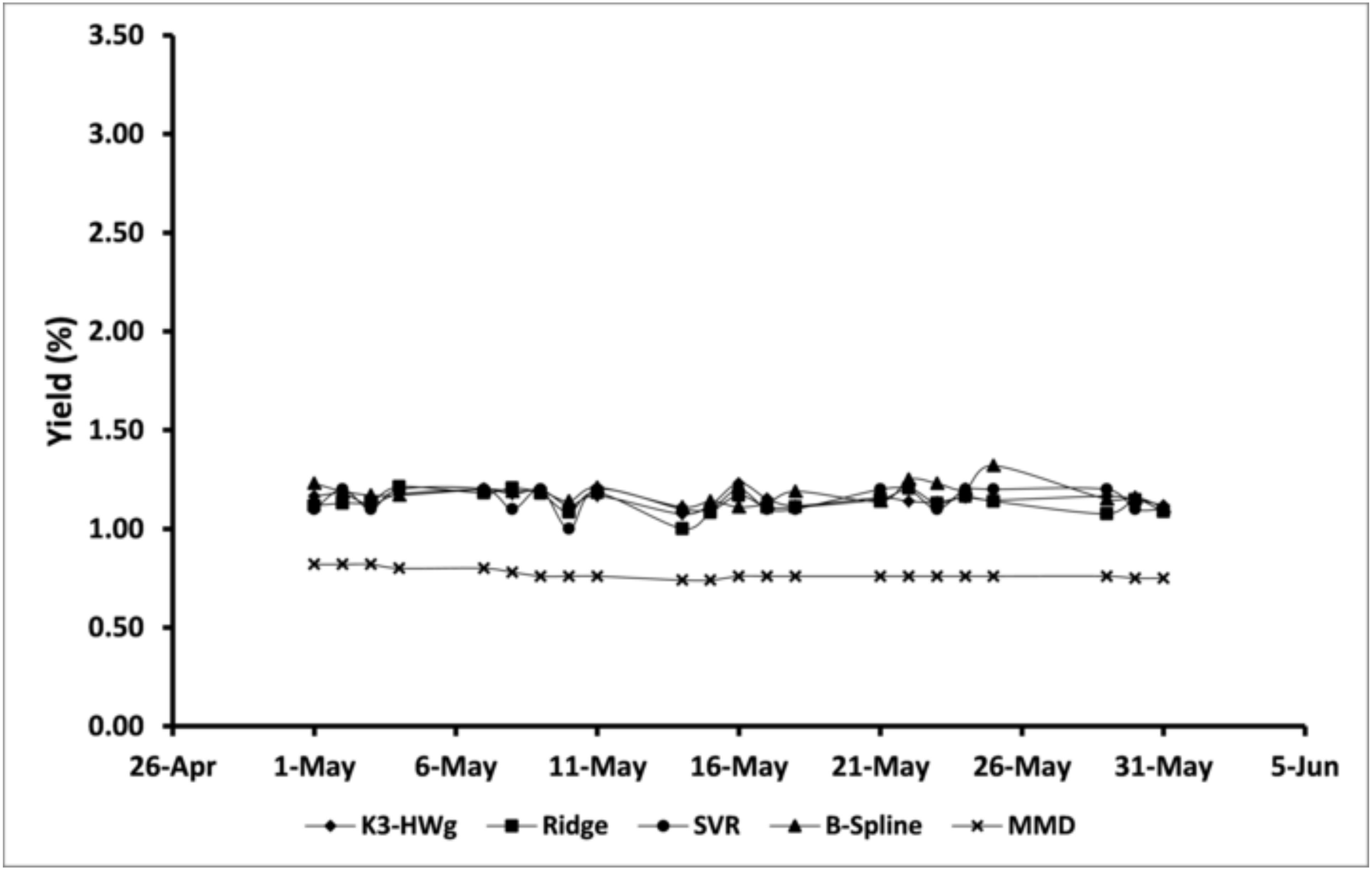

Figure 7B

Click here to download Figure Fig7B.png

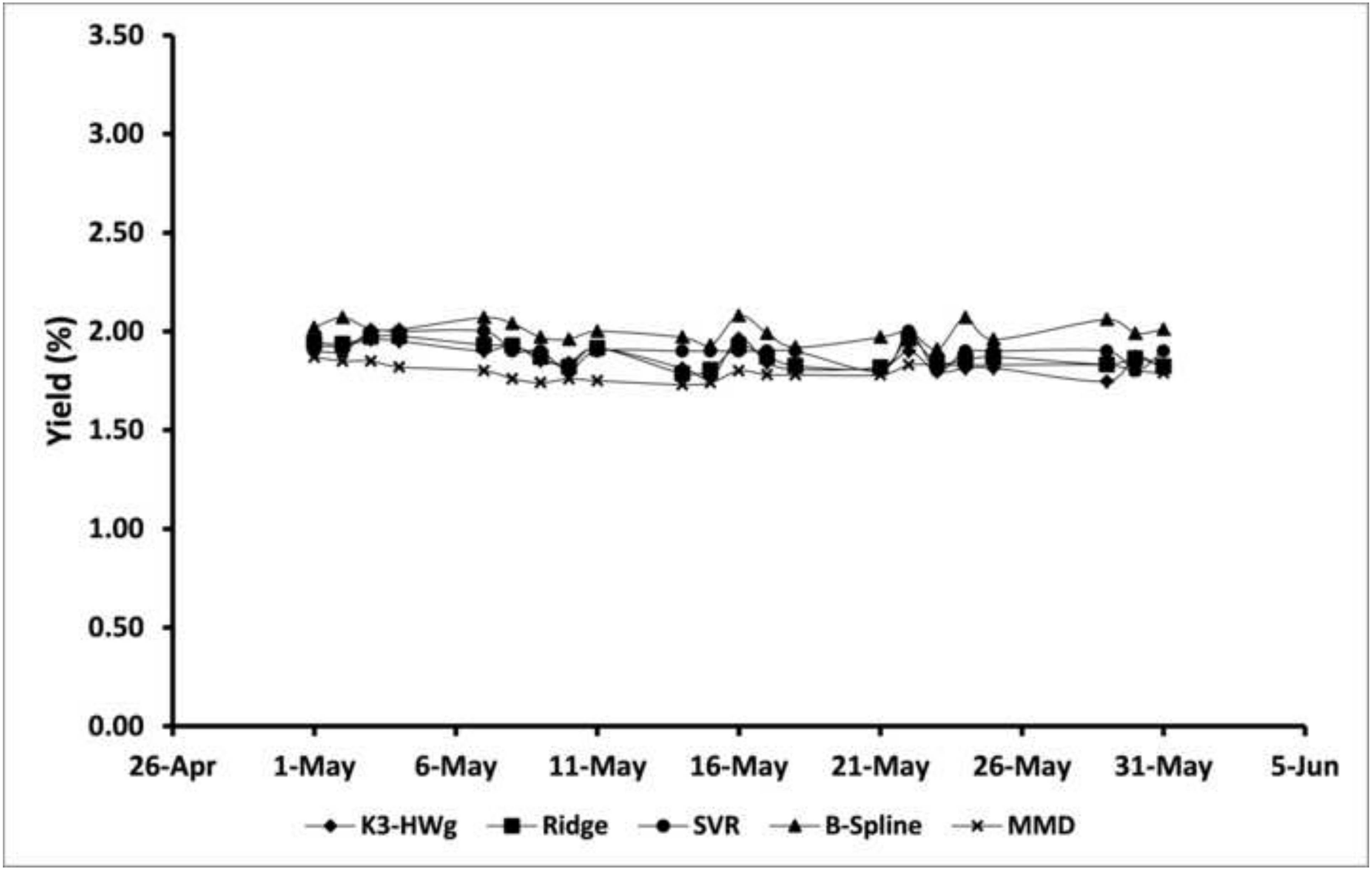

Figure 7C

Click here to download Figure Fig7C.png

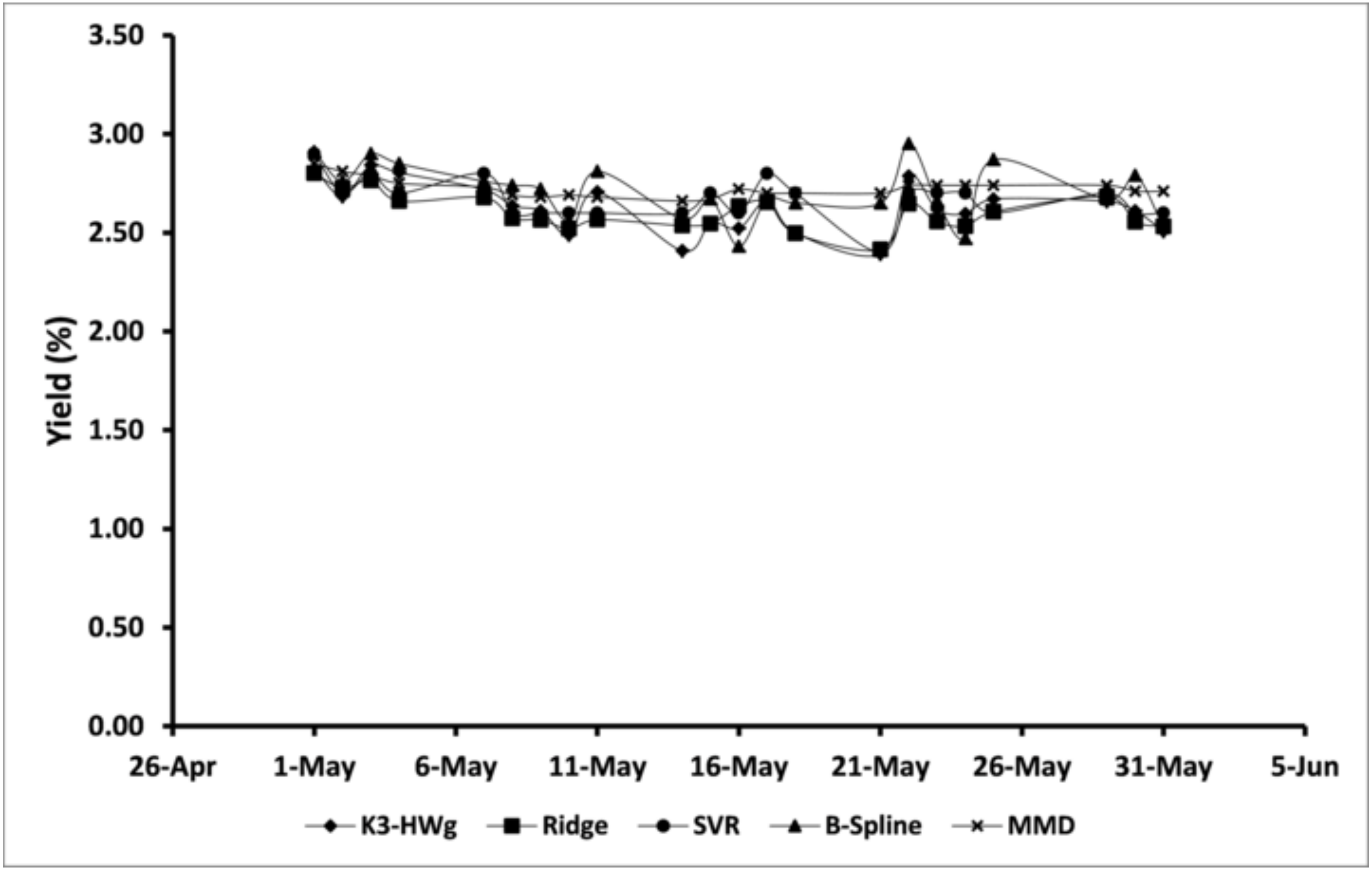

Figure 7D

Click here to download Figure Fig7D.png